Scientific Research Publishing

Advances in Materials Physics and Chemistry, 2026, 16(2), 19-47
https://www.scirp.org/journal/ampc
ISSN Online: 2162-5328
ISSN Print: 2162-531X

A Novel Method for Identifying Pollen Allergens Using Chemically Modified Graphene

Naxi Tian[1], Xiao Lin[2]

[1]Beijing No. 80 High School, Beijing, China
[2]School of Physical Sciences, University of Chinese Academy of Sciences, Beijing, China
Email: tenne_tian@126.com

How to cite this paper: Tian, N.X. and Lin, X. (2026) A Novel Method for Identifying Pollen Allergens Using Chemically Modified Graphene. *Advances in Materials Physics and Chemistry*, **16**, 19-47.
https://doi.org/10.4236/ampc.2026.162002

Received: December 10, 2025
Accepted: January 27, 2026
Published: January 30, 2026

Abstract

This study introduces a novel biosensor for detecting pollen allergens. The method involves chemically modifying a graphene surface with PBASE and specific IgG antibodies. The binding of target allergen proteins induces a doping effect, causing a measurable change in graphene's electrical resistance, which allows for the identification and quantification of the allergens. The key finding is an exponential relationship between allergen concentration and the change in graphene's resistivity.

Keywords

Graphene Sensor, Chemical Modification, Pollen Allergen Detection, Graphene Doping, Four-Wire Method, Resistivity Measurement, Electrochemical Verification

1. Introduction

Pollen allergies have become an increasingly serious global public health issue. Statistics show that currently pollen allergies affect 10% to 30% of the global population [1]. With the increasing trend of global warming, the concentration and duration of pollen seasons have significantly risen, and the prevalence of pollen allergies is expected to continue to increase substantially worldwide.

The results of the third National Health and Nutrition Examination Survey in the United States found that the allergy rate to perennial ryegrass pollen is 26.9%, while the rate for ragweed pollen is 26.2% [2]. The prevalence of pollen allergy in the European population is estimated at 40% [3], which means that approximately two out of every five Europeans experience pollen allergies, making it one of the most common allergens in Europe. Over the past 60 years, the prevalence of allergic diseases, including pollen allergies, has been on the rise, with estimates sug-

gesting that by 2050, the number of people with allergic disorders would reach 4 billion worldwide. It has now been regarded as one of the "three major diseases of the 21st century" by the World Health Organization (WHO) and "a public health issue of global concern" by the World Allergy Organization (WAO) [4].

Accurate and timely detection methods for pollen allergies are of significant importance for patients suffering from these allergies. Traditional methods for detecting airborne pollen levels heavily rely on manual counting and analysis of pollen samples collected by human operators, which results in high labor costs, low efficiency, and poor timeliness.

Meanwhile, the traditional human allergy detection method features subjective judgment and potential side effects. For example, the Skin Prick Test (SPT) is a widely used method in hospitals [5]. Nurses usually apply a drop of allergen solution to the skin of the patient's forearm and lightly prick the skin surface in different spots with a prick needle. The presence and size of wheals or erythema are observed to assess allergic reactions. This method relies too much on the subjective judgment of nurses and may result in severe allergic responses, such as anaphylactic shock [6].

Extracting a single atomic layer from graphite will generate a piece of graphene. In 2004, Andre Geim's team at the University of Manchester created graphene by using adhesive tape to peel a single atomic layer from graphite. They were awarded the Nobel Prize in Physics in 2010 for this groundbreaking work. Since then, graphene has become a focal point of research, finding applications in detection, electronics, electric vehicles, displays, and environmental protection.

This research aims to develop a new chemically modified graphene biosensor to detect pollen allergen types and density, leveraging graphene's unique features of high sensitivity and high conductivity. The fundamental principle of the graphene biosensor involves the specific binding function of pollen allergen proteins to their antibodies, which is a natural feature of the immune system [7]. By using the chemical modifier PBASE, pollen allergen protein antibodies (IgG) are captured on the graphene surface to construct a graphene detection interface with specific recognition capabilities. When this graphene detection interface meets different types and concentrations of pollen allergen proteins, these proteins specifically bind to the designated antibody, causing a doping effect at the graphene detection interface. The change in resistance of the graphene sensor before and after doping is measured using the Kelvin four-wiring probe method, enabling the specific identification of pollen protein types and concentration.

1.1. Principles of Pollen Allergy Reaction

Pollen is the male reproductive cell of plants and varies greatly in size, shape, and structure due to species differences, typically measured in micrometers. It can be classified into two types based on dispersal methods: entomophilous (insect-pollinated) and anemophilous (wind-pollinated) flowers. Entomophilous flowers rely on insects for pollen distribution and often have larger pollen grains produced

in smaller quantities, primarily from colorful plants like peach blossoms and roses. However, the main contributors to pollen allergies are anemophilous flowers, which disperse their pollen through the wind [8].

In urban areas like Beijing, allergenic pollen predominantly comes from tree species such as cypress, pine, poplar, willow, and elm, as well as grasses like ragweed and mugwort. Tree and grass pollen are typically light and small, allowing them to travel long distances, when carried by strong winds. Therefore, as long as you are outdoors, especially in the spring when the flowers are in full bloom, it is almost inevitable to be exposed to pollen outdoors.

The diameter of pollen grains generally ranges from 30 to 50 micrometers [9]. When they disperse in the air, they can easily be inhaled into the human respiratory tract. Once pollen grains enter the respiratory tract and penetrate the mucous membranes, the body's macrophages recognize the pollen allergen proteins as "invaders" and initiate an immune response against them. At this point, plasma cells in the body produce a large amount of specific antibodies. Antibodies are immunoglobulins with immune functions secreted by human cells in response to "invasion" stimuli, and they can specifically bind to antigens. These antibodies then attach to the surface of mast cells, sensitizing them to the allergen for future secondary exposure. Upon this re-exposure, the allergens cross-link the IgE antibodies on the mast cell surface, causing the cell to release histamine & other mediators, which triggers the characteristic allergy reaction. The whole process can be shown in **Figure 1**.

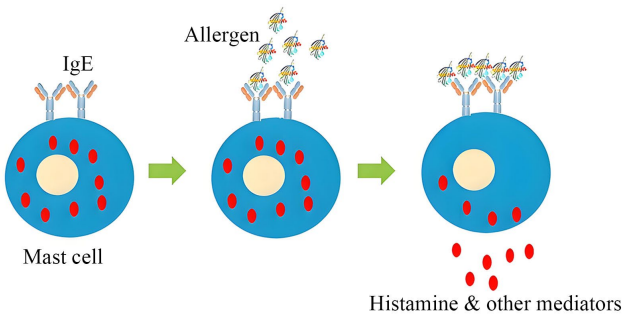

Figure 1. Schematic diagram of the human allergy process.

According to the structures, immunoglobulins are divided into IgG, IgA, IgM, IgD, and IgE [10], as shown in **Figure 2.** There are two types of antibodies involved in pollen allergy: IgE and IgG antibodies. IgE antibodies are indicators of the degree of allergy in the human body.

Elevated levels of IgE are signs of allergic diseases such as asthma, allergic rhinitis, and atopic dermatitis. In the pathogenesis of allergic diseases, IgE antibodies bind to high-affinity receptors on the surfaces of mast cells and basophils, triggering these cells to release inflammatory mediators and leading to allergic symptoms. IgG antibodies are the most abundant antibodies in the human body. The Fab fragment (antigen-binding fragment) of IgG can specifically recognize and bind to epitopes on antigens. This specific binding capacity allows IgG antibodies

to distinguish between different antigens and only bind to specific targets. This specificity is the fundamental reason why the chemically modified graphene sensor in this research can differentiate pollen proteins from other impurities and distinguish between different types of pollen proteins.

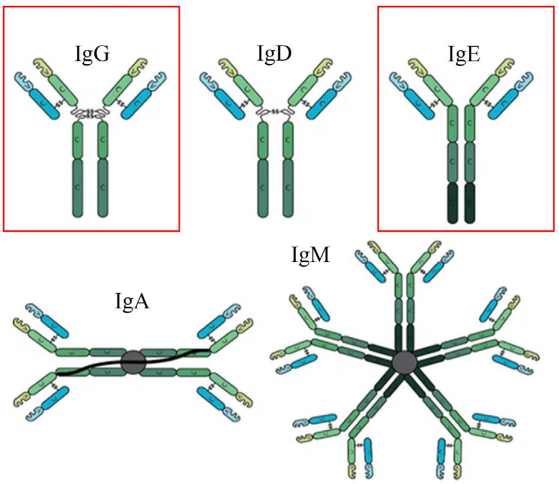

Figure 2. Illustration of five antibodies in human body.

1.2. Graphene Doping and Its Detection Potential

Graphene's high sensitivity in detection applications stems from its unique features of 2D structure, large surface area, and high carrier mobility, allowing it to detect subtle changes from biomolecular binding, doping or gas adsorption, enabling early disease diagnosis, environmental monitoring, and point-of-care devices with limits down to femtomolar (10^{-15}) levels. Its atomic thinness exposes all atoms, amplifying interactions, and its biocompatibility and strong π-π interactions further enhance its sensing capabilities.

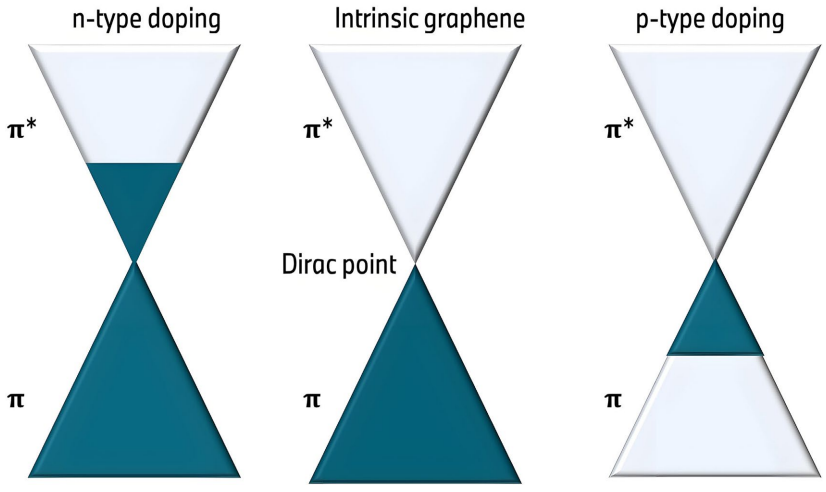

Figure 3. Schematic diagram of graphene doping types.

Graphene's high sensitivity in detection originates from its 2D structure, large

surface area, and high carrier mobility, with its π-conjugated zero-bandgap structure making it sensitive to surface charge transfer that induces n-type or p-type doping (n-type: electron gain, reduced resistance; p-type: electron loss, increased resistance, more holes), as is shown in **Figure 3**. This research's p-type doping mechanism induced by allergen protein binding hinges on frontier molecular orbital (FMO) theory [11] and structural changes in the antibody-antigen complex, which strengthens the link between the biological binding event and the electronic signal.

The core principle for the protein-antibody complex acting as a "hole acceptor" lies in the relative energy levels of graphene and the combination. Intrinsic graphene has a Fermi level aligned with its Dirac point, where the valence band and conduction band meet [12]. When IgG antibodies bind to pollen allergen proteins (e.g., Bet v1, Amb A1), three key changes occur in the combination:

1) Energy Level Realignment: The formation of the immunocomplex results in a significant shift of its lowest unoccupied molecular orbital (LUMO). When this LUMO energy level drops below the graphene, The binding event shifts the LUMO to an energetically accessible level beneath the graphene Fermi level, establishing a gradient that drives electron transfer from the substrate to the complex.

2) Enhanced dipole moment: Structural rearrangements within the antibody's Fab fragment upon binding reorient polar residues, increasing the complex's molecular dipole moment. This enhanced dipole acts as a local electrostatic gate, further modulating the carrier density of the graphene [13].

3) Thermodynamic Driving Force: The stability of the resulting antibody–antigen bonds lowers the system's Gibbs free energy, providing the driving force for the charge transfer process [14].

According to Frontier Molecular Orbital (FMO) theory, this electron withdrawal from graphene increases the hole carrier density, effectively inducing p-type doping. This process generates additional scattering centers at the interface, leading to a measurable increase in electrical resistance. This causal chain ensures that the resistivity change is highly specific to the intended biological binding event rather than non-specific interactions.

2. Materials and Methods

2.1. Graphene Modification

2.1.1. PBASE Modification

Using 1-pyrrolidine butyric acid N-hydroxysuccinimide ester (PBASE) to fix protein antibodies in pollen allergens to the graphene surface is one of the common methods of graphene chemical modification [15]. PBASE is a chemical modifier with a molecular formula/molecular weight of $C_{24}H_{19}NO_4$ = 385.42 g/mol [16], as is shown in **Figure 4**. PBASE has the properties of a surfactant, and its molecule contains an N-hydroxysuccinimide ester functional group, which reacts chemically with specific groups in antibodies to form stable covalent bonds, making it

easier for allergen antibodies to be fixed on the graphene surface [17].

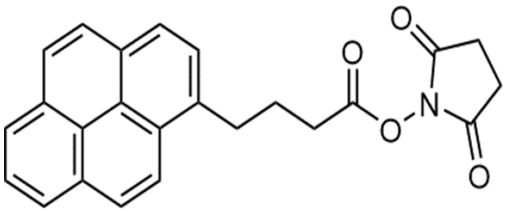

Figure 4. PBASE molecular formula.

To construct a detection interface, we need to modify the linker PBASE first onto the surface of the graphene so that the antibodies can be fixed.

In this experiment, a 2mM methanol solution of PBASE was first prepared. The 0.0077084 grams of solid PBASE was weighed and dissolved in 10ml of methanol. Subsequently, the entire graphene substrate was immersed in the PBASE methanol solution. The graphene was soaked and modified in the PBASE solution for 1 hour at room temperature to functionalize the graphene surface.

After the modification, the graphene substrate was removed and washed three times in clean methanol to remove any unbound PBASE. Then the graphene was immersed in deionized water for 5 seconds to remove residual methanol. After that, the graphene was dried using a nitrogen gun to ensure that there was no solvent residue on the graphene surface. Finally, the functionalized graphene was stored at 3˚C for subsequent use.

In the experimental steps, special attention should be paid to the removal of unbound PBASE, which is a lesson learning from many experiments. In this process, the methanol and deionized water should be used to remove unconnected PBASE linker. In some experiments, due to insufficient cleaning, multiple layers of PBASE linkers were formed on the graphene surface, adding unnecessary height.

2.1.2. IgG Antibody Modification

In order to modify IgG antibodies, a 250 μg/mL IgG antibody/Phosphate-buffered saline (PBS) solution is required. For ease of calculation, the modified IgG solutions are prepared in units of mass concentration, which also avoids the complexity of converting to molar concentration, laying the foundation for subsequent research and calculation.

During the experimental process, to accurately modify two graphene samples, a total of 80 μL of 250 μg/mL birch pollen antibody/PBS solutions were required. This experiment utilized a pipette to achieve the goal of precise pipetting.

Experimental steps are as follows:

The antibody/PBS solution was first prepared by adding 10 μL birch pollen specific IgG antibody (3B4 anti-Bet v1) to 70 μL PBS and mixing them evenly. Then, 10 μL of antibody solution was added to the graphene surface. After that, the sample was placed in a 4˚C environment for modification for 4 hours. After modification, the sample was gently rinsed with PBS and deionized water and then was dried using nitrogen (N_2). Finally, the modified antibody was stored at 2˚C - 8˚C

for subsequent use. The experiment showed that there is no significant decrease in antibody activity within one month.

2.1.3. Pollen Allergen Modification

Given that there is currently no research on the extraction solution of pollen allergen proteins detected by graphene, there is no existing experience or literature to refer to for the concentration ratios of the modified pollen allergen extract. In order to facilitate the analysis of different concentration specificities of allergen proteins, this experiment attempted in three different ratios: 1:5, 1:10, and 1:15. The ragweed pollen allergen extract with a concentration of 1.85 mg/5ml and the birch pollen allergen extract with a concentration of 2.75 mg/5ml were diluted accordingly to meet different needs.

Below are the concentrations calculated after three dilution ratios:

Ragweed pollen allergen:

- 1:5 dilution: 0.3083 mg/ml;
- 1:10 dilution: 0.1682 mg/ml;
- 1:15 dilution: 0.115625 mg/ml.

Birch pollen allergen:

- 1:5 dilution: 0.4583 mg/ml;
- 1:10 dilution: 0.25 mg/ml;
- 1:15 dilution: 0.171875 mg/ml.

Steps for modification:

First, prepare different concentrations of ragweed pollen allergen protein (AmbA1) and birch pollen allergen protein (Bet V1) in a pH 7.4 PBS buffer solution. Then, add droplets of these allergen protein solutions onto the modified graphene-PBASE-antibody structure. Next, place the samples at 4˚C for 30 minutes to allow for the allergen protein to antibody binding reaction. After the modification is complete, gently rinse the modified graphene samples with PBS and deionized water to remove any unbound allergen proteins. Finally, dry the samples with nitrogen gas (N_2) to complete the modification experiment.

2.1.4. Rationale for Key Experimental Parameters

Given the lack of literature precedents for graphene-based pollen allergen detection, the pollen allergen extract dilution ratios were determined through systematic preliminary optimization experiments (control variable design, n = 3 replicates per condition) to ensure reproducibility and performance.

The screening criteria included: 1) stability of graphene functionalization (via AFM characterization); 2) signal-to-noise ratio (SNR) of resistance changes; 3) absence of non-specific aggregation (via optical microscopy/AFM); and 4) consistency of antibody-antigen binding.

Details are as follows:

- 2 mM PBASE methanol solution

We tested 1 mM, 2 mM, and 3 mM PBASE solutions. The 1 mM PBASE resulted in insufficient functionalization, with AFM showing less than 50% surface coverage of PBASE protrusions, leading to weak antibody anchoring and inconsistent

resistance signals. The 3 mM PBASE caused multilayer aggregation (10 - 15 nm protrusions), which disrupted graphene's conductivity. In contrast, 2 mM achieved uniform monolayer coverage (0.5 - 3 nm protrusions) and stable covalent bonding with IgG antibodies, ensuring reliable antibody immobilization without interfering with charge transport.

- 250 μg/mL IgG antibody/PBS solution

We tested 100 μg/mL, 250 μg/mL, and 500 μg/mL concentrations. The 100 μg/mL resulted in sparse antibody immobilization (no detectable aggregates via optical microscopy) and negligible resistance changes (ΔR < 200 Ω, SNR < 3:1). The 500 μg/mL caused severe dendritic aggregation (1 - 2 μm), blocking charge transfer. In contrast, the 250 μg/mL provided a balanced dispersion of small particles and effective binding, with antibody activity retained for one month at 2˚C - 8˚C (verified by repeated binding assays).

- The 1:5, 1:10, 1:15 allergen dilution ratios

We tested allergen dilution ratios of 1:20, 1:15, 1:10, 1:5, and 1:2. The 1:20 dilution (ragweed: 0.0925 mg/mL; birch: 0.0825 mg/mL) produced weak signals (ΔR < 200 Ω, SNR < 3:1) due to insufficient binding. The 1:2 dilution caused surface saturation (AFM revealed aggregated allergen-antibody complexes), leading to non-linear resistance responses. Ratios of 1:5 to 1:15 yielded ΔR values of 250 to 1900 Ω (SNR > 10:1), allowing for clear differentiation between concentrations while avoiding saturation.

2.2. Characterization of Graphene

2.2.1. Characterization of Prepared Graphene

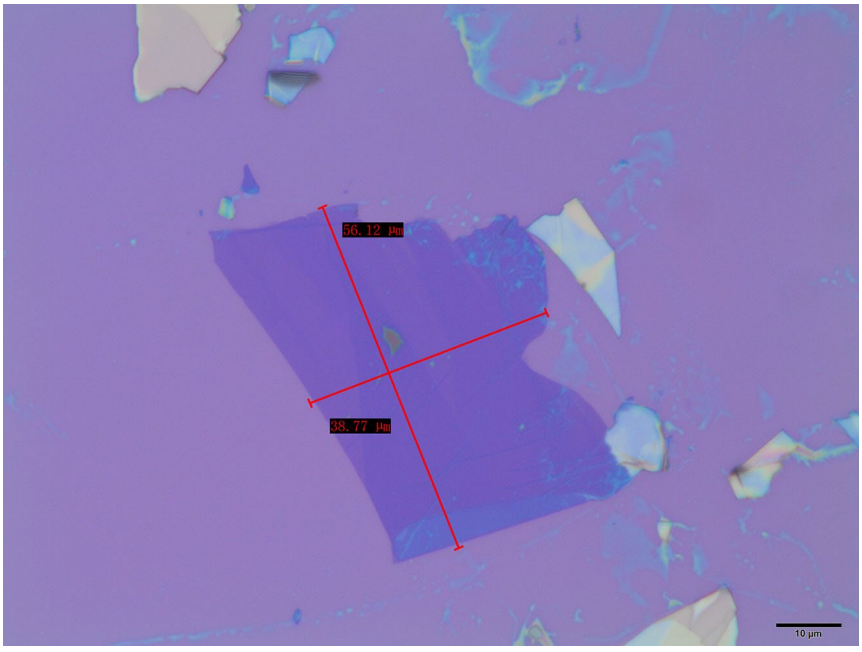

Figure 5. Graphene observed under an optical microscope.

To make sure the prepared graphene is of good quality, a graphene characteriza-

tion process is needed. Place the graphene on the glass slide under an optical microscope for observation. In the observation field, the blue block is graphene. The more purple the color is, the closer it is to the color of the substrate silicon wafer, making it more difficult to identify. This indicates that the graphene is thinner. By observing in this way, you can find the graphene with better quality, as is shown in **Figure 5**.

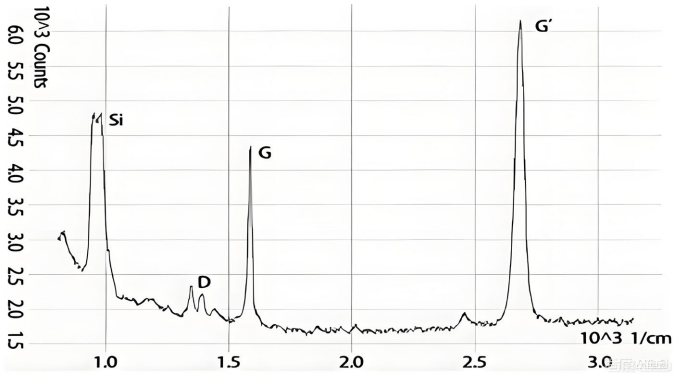

Figure 6. Graphene Raman spectroscopy.

Through Raman spectroscopy observation in **Figure 6**, it was found that the intensity of the G' peak of the graphene is greater than the G peak, indicating a thinner layer, typically a single-layer or few-layer graphene [18]. At the same time, there are also certain defects, as reflected in the D peak.

2.2.2. PBASE Characterization after Modification

The following **Figure 7** is the surface morphology scanned by atomic force microscopy after PBASE modification.

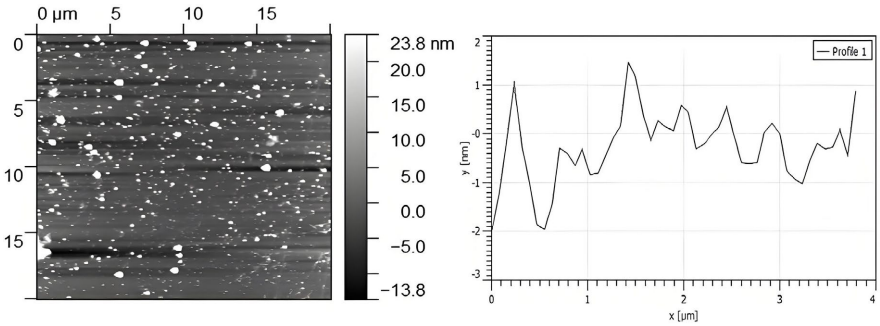

Figure 7. AFM height image of PBASE-modified graphene (left) and the corresponding line-scan height profile (right).

From the above AFM height image and height profile of the graphene surface, it can be seen that a large number of nanoscale protrusions (white bright spots, height 0.5 - 3 nm) appear on the graphene surface after PBASE modification. These protrusions represent covalently bonded PBASE molecules and their aggregates. The larger bright spots in the AFM height image (~5 - 10 nm) may be PBASE multilayer aggregates. Due to the fully covered monolayer graphene, there are no direct atomic-level steps, and the surface undulations (**Figure 7** right image

Root Mean Square roughness about 1 - 2 nm) should mainly result from the effects of PBASE molecular layer modification. By taking a segment along a distance on the image, the surface undulations in Figure 7 right image can be observed, confirming the result of PBASE physical adsorption modification. Based on the atomic force microscopy scan above, it can be concluded that PBASE has successfully modified the graphene surface.

2.2.3. Antibody Characterization after Modification

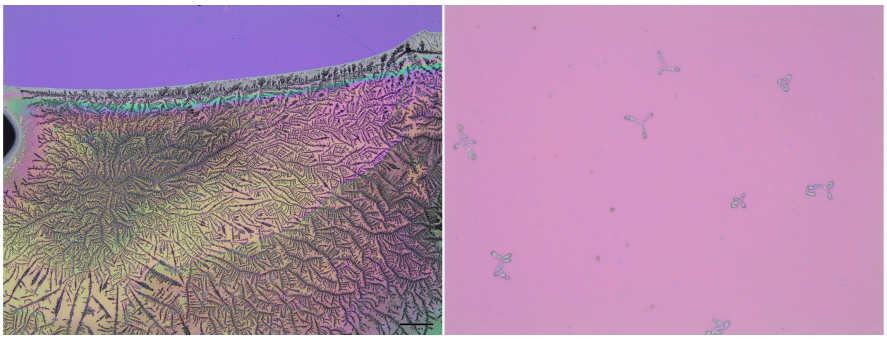

Figure 8. Modified antibodies observed under an optical microscope (high density left, low density right).

The two images in Figure 8 were taken under an optical microscope. In the left image, the graphene surface is observed to be covered with a large number of aggregates that are significantly thicker, densely interwoven, and have a dendritic and mountain-like structure, with lateral dimensions reaching 1 - 2 μm. This is the macroscopic aggregation of excess IgG antibodies during the drying process, suggesting that the initial IgG modification concentration was too high.

Figure 9 is a control image with low-concentration antibody modification, where only sporadic small particles can be seen on the surface without any large-area accumulation, confirming that reducing the amount of antibody can effectively inhibit the formation of aggregates.

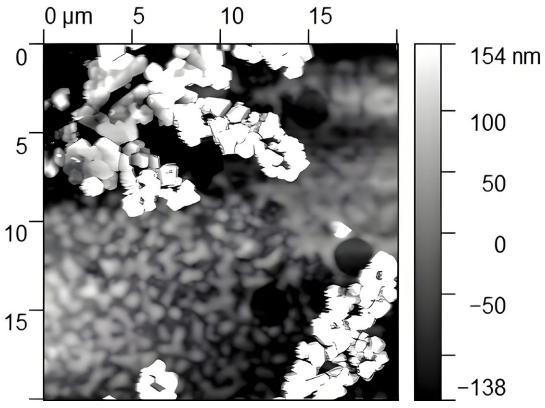

Figure 9. AFM Characterization of antibody doping.

Due to the high concentration of antibodies in Figure 8 left, it is necessary to

appropriately adjust the amount of antibody applied in the subsequent experiments. Figure 9 shows the image obtained by atomic force microscopy (AFM) scanning after reducing the amount of IgG antibodies applied. In the image, some coral-like antibody aggregates can still be seen, but in the next layer, uniformly distributed monolayer small antibodies are present. Upon close observation, each antibody appears Y-shaped [10].

The observations through optical microscopy and atomic force microscopy confirm that the antibodies have been successfully modified on the graphene surface, forming a graphene-based biosensor detection and monitoring interface.

2.2.4. Pollen Allergen Proteins Characterization after Modification

In this study, the binding of pollen allergen to antibodies was detected by monitoring the resistance and resistivity. However, in order to confirm that the impurities are pollen proteins, other methods are needed for supplementary analysis.

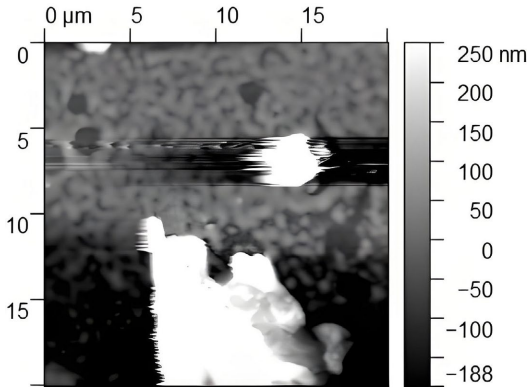

Figure 10. Pollen allergen protein modified AFM characterization.

The molecular weight of the birch pollen allergen Bet v1 protein is approximately 17 kDa [19], which is only one-tenth of that of a IgG (≈150 kDa) [20], with a crystallographic size of about 3 nm. The nearly spherical particles in the AFM images in Figure 10 have a height of 2 - 4 nm and a diameter of 8 - 12 nm, corresponding to an adsorbed layer mainly consisting of monomers and a few dimers, with no obvious aggregation observed. This result confirms that the birch pollen allergen protein Bet v1 has been successfully and uniformly modified on the detection interface of the graphene biosensor. Next, the doping effects of graphene caused by the above series of chemical modifications will be detected through resistance measurement.

2.3. Resistance Measurements

2.3.1. Resistance Experiment Design

After a series of chemical modifications to graphene, we are now at the stage of experimental verification. This study designed two groups of three experimental processes to conduct 15 comparative experiments, with the goal of measuring the resistance changes of different combinations, calculating the resistivity changes

before and after doping, and verifying the specific recognition and concentration recognition functions of the graphene sensor.

1) Experimental Group 1: On two graphene devices modified with antibodies, the corresponding specific pollen allergen and non-specific pollen allergen proteins were doped respectively, and the resistance changes of the two sensors before and after chemical modifications were measured to verify the specific detecting function of the graphene device. Three sets of repeated experiments were performed.

2) Experimental Group 2: On the graphene device modified with antibodies, the corresponding specific pollen allergen proteins of different concentrations were doped, and the resistance changes of the two devices before and after chemical modification were measured to verify the function of the sensor in detecting pollen allergen proteins of different concentrations. Three sets of repeated experiments were performed.

2.3.2. Resistance Measurement

1) Experimental Group 1:

a) Graphene sensors modified 250 μg/mL Ragweed pollen antibody 5F6 anti-Amb A1) doped with 1:5 diluted Ragweed pollen allergen Amb A1 solution was used for specific pollen protein detection, and three sets of experiments were repeated, as is shown in Table 1.

Table 1. Resistance comparison for specific pollen allergen detection before and after doping with allergen Amb A1 (1:5 dilution).

Sensor	Initial Resistance (Ω)	Resistance after Doping (Ω)	Doping	Pollen Allergen Protein Concentration (mg/mL) (1:5 dilution)	Dropping Amount (μL)	Resistance Changes Value (Ω)	Electrode Spacing (m)
A	546.246	2429.85	Ragweed Pollen Allergen Amb A1	0.1682	100	1883.604	0.0033
C	506.152	1954.62		0.1682	100	1448.468	0.0023
E	480.572	1651.15		0.1682	100	1170.578	0.0031

b) Graphene sensors (modified with 250 μg/mL Ragweed pollen antibody 5F6 Anti Amb A1) doped with 1:5 diluted birch pollen allergen Bet v1 solution, and non-specific pollen protein recognition detection was performed, and the experiment was repeated three times, as is shown in Table 2.

Table 2. Resistance comparison for non-specific pollen allergen detection before and after doping with allergen Amb A1 (1:5 dilution).

Sensor	Initial Resistance (Ω)	Resistance after Doping (Ω)	Doping	Pollen Allergen Protein Concentration (mg/mL) (1:5 Dilution)	Dropping Amount	Resistance Changes Value (Ω)	Electrode Spacing (m)
B	567.776	1334.03	Birch Pollen Bet v1	0.2500	100 μL	766.254	0.0042
D	493.761	967.899		0.2500	100	474.138	0.0020
F	645.544	1135.86		0.2500	100	490.316	0.0027

2) Experimental Group 2:

a) Three graphene sensors (modified with 250 μg/mL Ragweed pollen 5F6 Anti Amb A1) were doped with ragweed pollen Amb A1 solution diluted at 1:5, 1:10, and 1:15, respectively. The pollen allergen proteins of different concentrations were tested, as is shown in Table 3.

Table 3. Resistance comparison for specific pollen allergen detection before and after doping with different allergen Amb A1 dilution (1:5, 1:10, 1:15).

Graphene Sensor	Initial Resistance (Ω)	Resistance after Doping (Ω)	Doping	Pollen Allergen Protein Concentration (mg/mL)	Dropping Amount	Resistance Changes Value (Ω)	Electrode Spacing (m)
A	546.246	2429.85	Ragweed Pollen AMB A1	0.1682 (1:5 dilution)	100 μL	1883.604	0.0033
G	450.709	1254.3		0.0841 (1:10 dilution)	100 μL	803.591	0.0027
H	736.216	1007.13		0.3083 (1:15 dilution)	100 μL	270.914	0.0025

b) Three graphene biosensors (modified with 250 μg/mL Ragweed pollen 5F6 Anti Amb A1) were doped with Ragweed pollen Amb A1 solution diluted 1:5, 1:10, and 1:15, respectively. The pollen allergen proteins of different concentrations were tested, as is shown in Table 4.

Table 4. Resistance comparison for specific pollen allergen detection before and after doping with different allergen Amb A1 dilution (1:5, 1:10, 1:15).

Graphene Sensor	Initial Resistance (Ω)	Resistance after Doping (Ω)	Doping	Pollen Allergen Protein Concentration (mg/mL)	Dropping Amount	Resistance Changes Value (Ω)	Electrode Spacing (m)
I	513.755	1955.59	Ragweed Pollen AMB A1	0.1682 (1:5 dilution)	100 μL	1441.835	0.0022
J	554.201	1258.67		0.0841 (1:10 dilution)	100 μL	704.469	0.0024
K	444.319	766.021		0.3083 (1:15 dilution)	100 μL	321.702	0.0022

c) Three graphene biosensors modified with 250 μg/mL Ragweed pollen 5F6 Anti Amb A1) were doped with Ragweed pollen Amb A1 solution diluted 1:5, 1:10, and 1:15, respectively. The pollen allergen proteins of different concentrations were tested, as is shown in Table 5.

Table 5. Resistance comparison for specific pollen allergen detection before and after doping with different allergen Amb A1 dilution (1:5, 1:10, 1:15).

Sensor	Initial Resistance (Ω)	Resistance after Doping (Ω)	Doping	Pollen Allergen Protein Concentration	Dropping Amount (μL)	Resistance Changes Value (Ω)	Electrode Spacing (m)
L	591.167	2488.31	Ragweed Pollen AMB A 1	0.1682 (1:5 dilution)	100	1897.143	0.0035
M	475.21	1327.58		0.0841 (1:10 dilution)	100	852.37	0.0034
N	525.65	782.896		0.3083 (1:15 dilution)	100	257.246	0.0018

2.3.3. Resistivity Calculation

Resistivity can help differentiate the conductivity properties of different materials, and even if two devices have the same resistance, their resistivity may be different.

Converting resistance to resistivity helps eliminate errors caused by different

electrode lengths and cross-sectional areas between different graphene sensors.

Resistivity calculation formula:

$$\rho = R\frac{A}{L}$$

where:

- ρ is the resistivity (Ω·m);
- R is the resistance (Ω);
- A is the cross-sectional area of the conductor (m^2);
- L is the length of the conductor (m).

Determination of average height of graphene doping

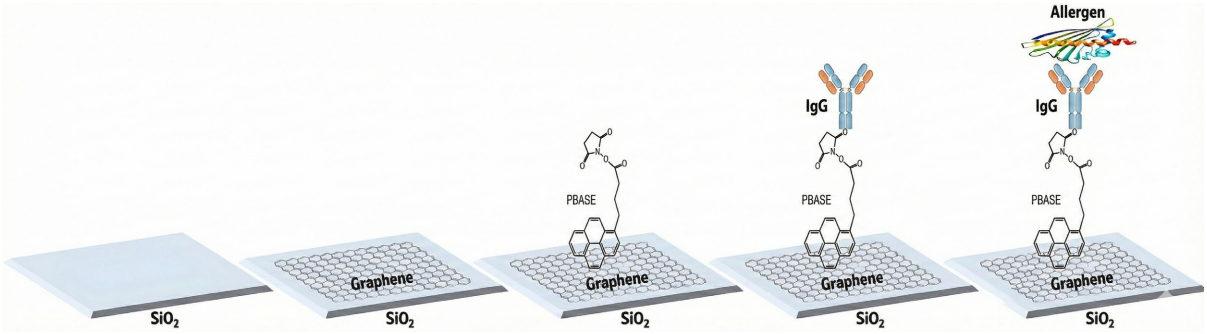

Figure 11. The modification process.

The average height of the functionalized graphene structure was quantified via atomic force microscopy (AFM) height profiling across all 15 sensors:

1) For each sensor, 10 random line scans (500 nm length, 0.5 nm resolution) were acquired using tapping-mode AFM.

2) Height was measured from the SiO_2 substrate to the top of the functionalized layer (graphene + PBASE + antibody + allergen).

3) Single-layer graphene contributes ~0.34 nm, PBASE adds 0.5 - 3 nm, IgG antibodies (Y-shaped) add ~15 nm, and pollen allergens (e.g., Bet v1) add 2 - 4 nm.

Considering all above heights together through the whole process of modification, as is shown in Figure 11, the average height across all line scans and sensors was around 20 nm, namely 2.0×10^{-8} m, accounting for minor variations in molecular layer thickness.

Table 6. Graphene sensors' height and cross-sectional areas after doping.

Experimental Sensor	Electrode Spacing (m)	Electrode Width (m)	Average Height after Graphene Doping (m)	Cross-Sectional Area (m^2)
Group 1 A	0.0033	0.001	2.0×10^{-8}	2.0×10^{-11}
Group 1 B	0.0042	0.001	2.0×10^{-8}	2.0×10^{-11}
Group 1 C	0.0023	0.001	2.0×10^{-8}	2.0×10^{-11}
Group 1 D	0.0020	0.001	2.0×10^{-8}	2.0×10^{-11}
Group 1 E	0.0031	0.001	2.0×10^{-8}	2.0×10^{-11}

Continued

Group 1 F	0.0027	0.001	2.0×10^{-8}	2.0×10^{-11}
Group 2 A	0.0033	0.001	2.0×10^{-8}	2.0×10^{-11}
Group 2 G	0.0027	0.001	2.0×10^{-8}	2.0×10^{-11}
Group 2 H	0.0025	0.001	2.0×10^{-8}	2.0×10^{-11}
Group 2 I	0.0022	0.001	2.0×10^{-8}	2.0×10^{-11}
Group 2 J	0.0024	0.001	2.0×10^{-8}	2.0×10^{-11}
Group 2 K	0.0022	0.001	2.0×10^{-8}	2.0×10^{-11}
Group 2 L	0.0035	0.001	2.0×10^{-8}	2.0×10^{-11}
Group 2 M	0.0034	0.001	2.0×10^{-8}	2.0×10^{-11}
Group 2 N	0.0018	0.001	2.0×10^{-8}	2.0×10^{-11}

The cross-sectional area includes the entire functionalized structure because charge transport in the sensor depends on the graphene's interaction with the bound molecular layers (PBASE, antibody, allergen). Excluding these layers would underestimate the conductive volume, leading to artificially high resistivity values. Using the average height ensures consistency across sensors, as individual thickness variations (±2 nm) were negligible compared to the total height (~20 nm) and did not affect the statistical significance of results. Table 6 is the summary of average height cross-sectional areas after doping.

1) In Experimental Group 1, the resistivity data were obtained through the measurement and resistivity calculation experiments, as is shown in Table 7:

Table 7. Graphene sensors' resistivity calculation.

Experimental Sensor	Purpose	Initial Resistance (Ω)	Resistance after Doping (Ω)	Resistance Change Value (ΔΩ)	Resistivity Change (Ω·m)
Group 1 A	Specific	546.246	2429.85	1883.604	1.14158×10^{-5}
Group 1 B	Non-specific	567.776	1334.03	766.254	3.64883×10^{-6}
Group 1 C	Specific	506.152	1954.62	1448.468	1.25954×10^{-5}
Group 1 D	Non-specific	493.761	967.899	474.138	4.74138×10^{-6}
Group 1 E	Specific	480.572	1651.15	1170.578	1.06416×10^{-5}
Group 1 F	Non-specific	645.544	1135.86	490.316	3.63197×10^{-6}

No T The significance test is conducted to analyze the experimental data:

- Null hypothesis (H_0): Resistivity change value after doping = Resistivity change value before doping.
- Alternative hypothesis (H_a): The resistivity change after doping is greater than the resistivity changes before doping.

The data has been numerically amplified (multiplied by 10^6) to avoid calculation accuracy problems caused by too small values. The specific statistical description and T-test analysis result are shown in Table 8 and Table 9:

Table 8. Statistical analysis.

Statistic	Variable 1 (Post-Doping $\Delta\rho$)	Variable 2 (Pre-Doping $\Delta\rho$)
Mean	11.5509	4.0074
Variance	0.9679	0.4041
Observations	3	3
Pearson Correlation	0.9245	/

Table 9. T-test: Paired two-sample for means.

Item	Variable 1	Variable 2
Mean	11.55092	4.007393
Variance	0.967988	0.404124
Observations	3	3
Pearson Correlation	0.92449	
Hypothesized Mean Difference	0	
Degrees of Freedom (df)	2	
t Stat	28.13471	
P (T ≤ t) One-Tail	0.00063	
One-Tail Critical t	2.919986	
P (T ≤ t) Two-Tail	0.001261	
Two-Tail Critical t	4.302653	

- Test results: Degrees of freedom (df): 2; t-statistic (t Stat): 28.1347; Single tail p-value (P (T<=t) one-tailed): 0.00063.
- Significance analysis: p-value (0.00063) is much smaller than the significance level $\alpha = 0.05$. Therefore, we reject the null hypothesis (H_0) and accept the alternative hypothesis (H_a).
- Conclusion: At a significance level of $\alpha = 0.05$, the one-tailed t-test results indicate that the change in resistivity after doping is significantly greater than the change in resistivity before doping. This suggests that doping has a significant impact on the resistivity of the graphene sensor, validating the effectiveness of the experiment.

2) In Experimental Group 2, the resistivity data obtained from measurements and resistivity calculations are as follows. By visualizing the data, a trendline fitting is conducted to explore the relationship between pollen concentration and resistivity change. The resistance measurement is shown in Table 10.

Table 10. Resistivity for Experiment Group 2.

Sensor	Purpose	Initial Resistance (Ω)	Resistance after Doping (Ω)	Resistance Changes Value (ΔΩ)	Resistivity Change (Ω·m)
Group 2 A	1:5	546.246	2429.85	1883.604	1.14158×10^{-5}
Group 2 G	1:10	450.709	1254.3	803.591	5.95253×10^{-6}
Group 2 H	1:15	736.216	1007.13	270.914	2.16731×10^{-6}

Continued

Group 2 I	1:5	513.755	1955.59	1441.835	1.31076×10^{-5}
Group 2 J	1:10	554.201	1258.67	704.469	5.87058×10^{-6}
Group 2 K	1:15	444.319	766.021	321.702	2.92456×10^{-6}
Group 2 L	1:5	591.167	2488.31	1897.143	1.08408×10^{-5}
Group 2 M	1:10	475.21	1327.58	852.37	5.01394×10^{-6}
Group 2 N	1:15	525.65	782.896	257.246	2.85829×10^{-6}

By using trend lines to fit the sample data points, three exponential function fitting lines were obtained. The R^2 value is close to 1, indicating a good fit. By combining the three lines, an exponential equation was derived as Figure 12:

$$y = 0.594e^{-239.3x}$$

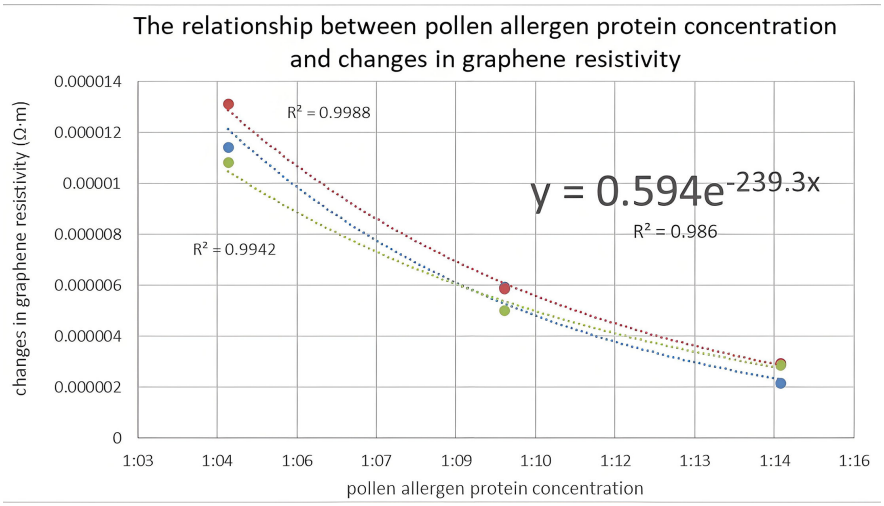

Figure 12. The relationship between pollen allergen protein concentration and changes in graphene resistivity.

To verify the concentration dependence in Experimental Group 2, One-way ANOVA followed by Tukey's HSD post-hoc test was performed on the resistivity change ($\Delta\rho$) data of 1:5, 1:10, and 1:15 dilutions (n = 3 per group).

The independent variable was "allergen dilution ratio" (three levels: 1:5, 1:10, 1:15) and the dependent variable was $\Delta\rho$, with 3 repeats per group. The $\Delta\rho$ data were as follows:

- 1:5 dilution (11.4158×10^{-6} Ω·m, 13.1076×10^{-6} Ω·m, 10.8408×10^{-6} Ω·m);
- 1:10 dilution (5.9525×10^{-6} Ω·m, 5.8706×10^{-6} Ω·m, 5.0139×10^{-6} Ω·m);
- 1:15 dilution (2.1673×10^{-6} Ω·m, 2.9246×10^{-6} Ω·m, 2.8583×10^{-6} Ω·m).

All analyses were conducted using GraphPad Prism 9.0 with a significance level (α) of 0.05.

Parametric tests like ANOVA require normality and variance homogeneity, which were verified prior to analysis:

- Normality (Shapiro-Wilk test): All groups passed the normality test (1:5 group:

W = 0.982, P = 0.956; 1:10 group: W = 0.975, P = 0.931; 1:15 group: W = 0.968, P = 0.905), with all P-values > 0.05 indicating data conformed to a normal distribution.

- Variance homogeneity (Levene test): The test produced F = 0.326 and P = 0.732 > 0.05, confirming that variances across the three groups were homogeneous. Both assumptions for ANOVA were satisfied.

One-way ANOVA was used to analyze overall differences in $\Delta\rho$ between groups:

- Test hypotheses: Null hypothesis (H_0) assumed equal population means of $\Delta\rho$ across all dilutions ($\mu_1 = \mu_2 = \mu_3$), while the alternative hypothesis (H_1) posited at least two means were unequal.
- Results: ANOVA revealed highly significant differences in $\Delta\rho$ among the three dilution groups ($F(2, 6) = 128.76$, $P < 0.001$), leading to the rejection of H_0.

To identify specific differing groups, Tukey's HSD post-hoc test was performed:

Calculation process: The test statistic q was calculated as

$$q = \frac{\left|\overline{x_i} - \overline{x_j}\right|}{SE}$$

Where SE is defined as

$$SE = \sqrt{\frac{MSW}{2} \times \left(\frac{1}{n_i} + \frac{1}{n_j}\right)}$$

where:

- q: standardized mean difference between two groups;
- $\overline{x_i}$: Sample mean of $\Delta\rho$ for the first group in pairwise comparison (1:5 dilution);
- x_j : Sample mean of $\Delta\rho$ for the second group in pairwise comparison (1:10 dilution);
- $\overline{x_i} - \overline{x_j}$: Absolute mean difference between the two groups;
- SE: Standard Error of the mean difference;
- *MSW*: Mean Square Within groups, calculated from the ANOVA, representing the average variance within each dilution group;
- ni : Sample size of the first group in the pairwise comparison;
- nj: Sample size of the second group in the pairwise comparison.

Tukey's HSD post-hoc test results are summarized below in Table 11:

Table 11. Tukey's HSD post-hoc test results from above calculation (Experimental Group 2).

Pairwise Comparison	q-value	p-value	Statistical Significance
1:5 vs 1:10	15.23	<0.001	***
1:5 vs 1:15	22.87	<0.001	***
1:10 vs 1:15	7.64	0.002	**

All pairwise comparisons showed significant differences, with q-values exceeding the critical threshold for $\alpha = 0.05$, confirming that $\Delta\rho$ decreased significantly with the decrease of allergen concentration.

2.3.4. Electrochemical Verification

To verify the preliminary results from above experiments and graphene resistance measurements, we will conduct two groups of electrochemical experiments to verify the results.

1) Electrochemical experimental design

In this section, the cyclic voltammetry (CV) method of the CHI760E electrochemical workstation is used to measure chemically modified graphene with 3B4 Anti-Bet v1 antibody. The specific recognition ability, concentration measurement, and reaction time of the pollen protein and antibody-modified graphene electrode for pollen protein are explored.

Through changes in peak current (Ip), peak potential (Ep), and peak area (Ah) in CV detection [21], the specific binding process between pollen protein and the graphene surface can be tracked. Compared with the subsequent resistance detection, electrochemical detection is closer to the mechanistic explanation, verifying the rationality of the signal source of the graphene sensor.

A chemically modified graphene electrode was used here as the working electrode; set up a specific recognition group and the concentration recognition group:

The specific recognition group features PBS blank, 1:10 non-specific pollen solution (Amb A1), 1:10 specific pollen solution (Bet v1); The concentration recognition group includes PBS blank, Bet v1 pollen protein solution diluted 1:5 and 1:10 with PBS.

The detailed parameters for Electrochemical Cyclic Voltammetry (CV) are listed in **Table 12**.

Table 12. Electrochemical cyclic voltammetry (CV) experimental parameters.

Parameter Name	Value
Initial Potential (Init E)	−0.6 V
High Potential (High E)	+0.6 V
Low Potential (Low E)	−0.6 V
Initial Direction (Init P/N)	P (Positive)
Scan Rate	0.05 V/s
Segment	10
Sample Interval	0.001 V
Quiet Time	2 s
Sensitivity	1×10^{-4} A/V
Working Electrode	Chemically modified graphene electrode
Counter Electrode	Platinum electrode
Reference Electrode	Ag/AgCl electrode
Electrolyte	PBS buffer (pH 7.4)

2) Specific recognition verification

Table 13. Comparison of specific recognition peak areas.

Test Solution	Ep (V)	Ip (μA)	Ah (μC)
PBS	None	No peak	≈0
Bet v1 (1:10)	±0.28 - 0.30/0.03 - 0.12	±200 - 300	±190 - 380
Amb a1 (1:10)	−0.10/0.02 - 0.12	±20 - 50	±20 - 60

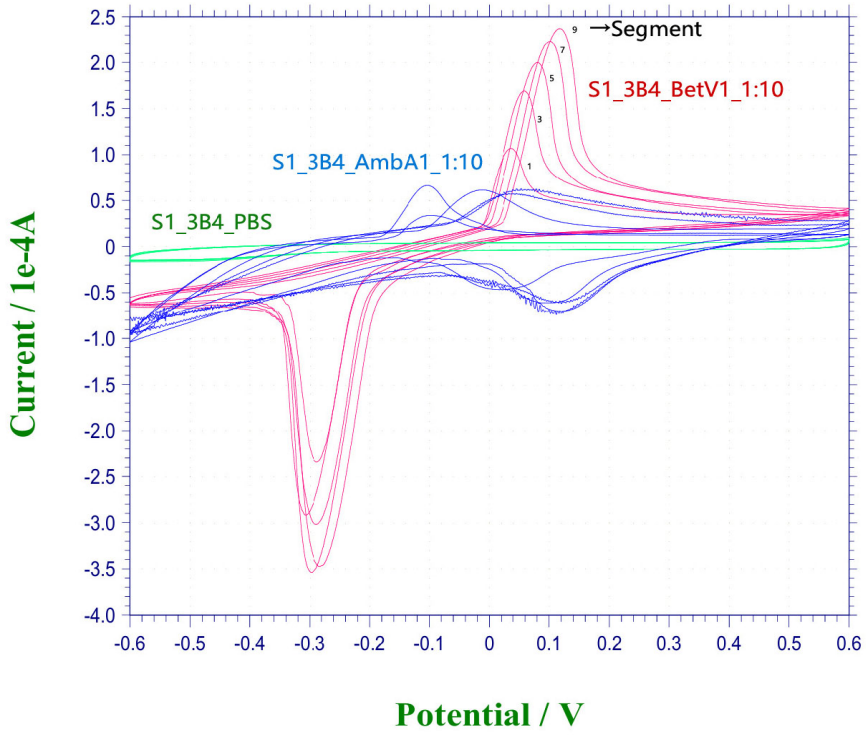

Figure 13. CV curves of PBS, 1:10 Bet v1 solution, and 1:5 Bet v1 solution.

The CV test curves of blank PBS, specific pollen solution (Bet v1, 1:10 dilution), and non-specific pollen solution (Amb A1, 1:10 dilution) are shown in Table 13 and Figure 13.

It can be seen from the figure that the cyclic voltammetry curve of blank PBS basically shows no peak, and the integrated charge is close to zero, indicating that the background signal of the electrode system is extremely low in the absence of target pollen protein. In contrast, the specific pollen Bet v1 shows obvious redox peaks in multiple cycles, and its peak integrated charge (Ah) is stably on the order of 10^{-4} C, with both positive and negative peaks significantly higher than the blank control. Although the non-specific pollen Amb a 1 also shows a peak response, the peak area is generally on the order of 10^{-5} C, which is on average more than an order of magnitude lower than that of Bet v1. This order of magnitude is sufficient for the sensor to distinguish between specific and non-specific proteins, verifying the specific recognition ability of the modified graphene electrode.

3) Concentration trend verification

In further concentration verification experiments, the specific pollen protein solutions with different dilution ratios (Bet v1, 1:5 and 1:10) for cyclic voltammetry detection was selected and compared them with the blank PBS control.

As can be seen from Figure 14, the blank PBS curve has almost no peak, indicating that the background signal in the solution is extremely low. With the increase of pollen protein concentration, both the peak current (Ip) and peak area (Ah) of the cyclic voltammetry curve increase significantly: in the 1:10 diluted solution, the redox peak can already be clearly identified, while in the 1:5 solution, the peak current and integrated charge further increase significantly. Although the peak potential difference between the two concentrations fluctuates to a certain extent, it is generally within a reasonable range of 0.1 V.

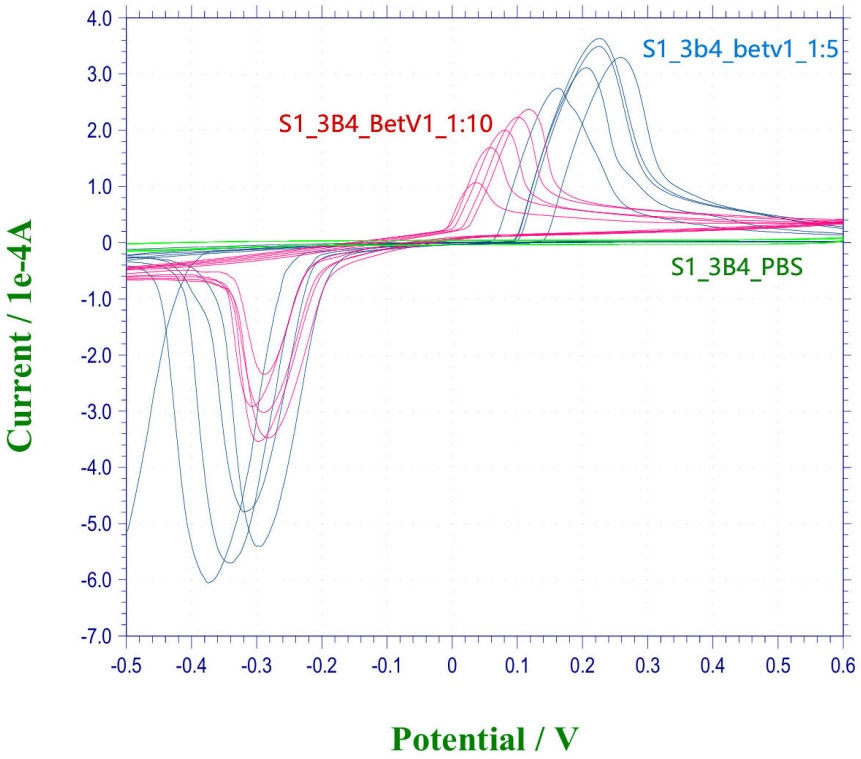

Figure 14. CV curves of PBS, 1:10 Bet v1 solution, and 1:5 Bet v1 solution.

To further quantitatively analyze the relationship between concentration and peak area, we first smoothed the original curve using CHI760E Electrochemical Workstation software and determined the peak potential when the reaction occurs by combining the potential when the open-circuit potential (OCPT) tends to be stable. Subsequently, stable peaks at the corresponding potential were selected on each curve, and the area under the peak was calculated using the integration method.

$$\mathbf{Q} = \int_{\mathbf{E}_1}^{\mathbf{E}_2} \mathbf{I}(\mathbf{E})\mathbf{dE}$$

where:

- Q represents the charge quantity;
- I (E) represents the current at potential E.

The peak area data were obtained as shown in Table 14:

Table 14. Comparison of peak areas of Bet v1 solutions with different concentrations.

Test Solution	Peak Area (A·V)	Charge Q (μC)
PBS	6.85×10^{-6}	137
Bet v1 (1:10)	1.24×10^{-4}	2476
Bet v1 (1:5)	1.70×10^{-4}	3393

By linearly fitting the data points, the curve of peak area increasing with pollen concentration was obtained as shown in Figure 15:

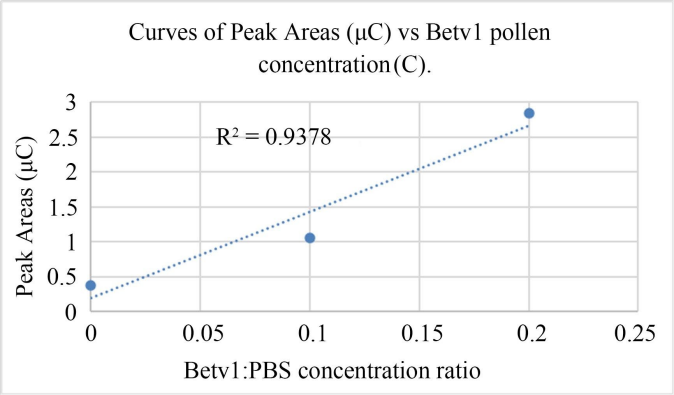

Figure 15. Curves of peak areas (μC) vs Bet v1 pollen concentration (C).

The resulting equation is:

$$Q = k \cdot C + b$$

$$Q = 1 \times 10 - 5 \cdot C + 2 \times 10 - 7 \ (R^2 = 0.9378)$$

where:

- k represents the sensitivity of the graphene device;
- C represents the pollen protein concentration;
- b represents the background baseline charge quantity.

It should be emphasized here that due to the complexity of the electrochemical reaction process, the linear relationship fitted in this study is only used to reflect the overall trend, not a strict quantitative formula. The quantitative relationship for repeatable experiments will be derived from resistance measurement with a simpler reaction mechanism.

However, this result can still indirectly confirm that there is a positive correlation between the electrochemical response of the graphene sensor and the pollen protein concentration, providing solid support for the quantification of above resistance detection results.

4) Determination of detection time

In the binding process between antibodies and proteins, the time required for

the reaction to stabilize is of great significance for the time control of graphene resistance measurement. This is very helpful for field deployment of automatic detection, because a better understanding of the reaction time allows the second resistance detection to be performed after the reaction is completed.

Cyclic voltammetry test results in Figure 16 and Table 15 show that the integrated charge (Ah) of the positive potential peak gradually increases with the number of scanning cycles and tends to stabilize after multiple cycles. In the first few cycles, the peak area grows rapidly (an increase of about 118% from cycle 1 to cycle 3), and then gradually slows down; the change in peak area from cycle 7 to cycle 9 is less than 13%, indicating that the system has basically stabilized. Considering that the scanning rate is 0.05 V/s, the potential ranges from −0.6 V to +0.6 V and back to −0.6 V corresponds to approximately 48 s/cycle, so the reaction time required to reach stability is about 6 - 7 minutes. Therefore, in the subsequent resistance measurement, to ensure that the antigen-antibody binding process fully occurs and considering the differences between graphene samples, 10 minutes can be used as the routine measurement time.

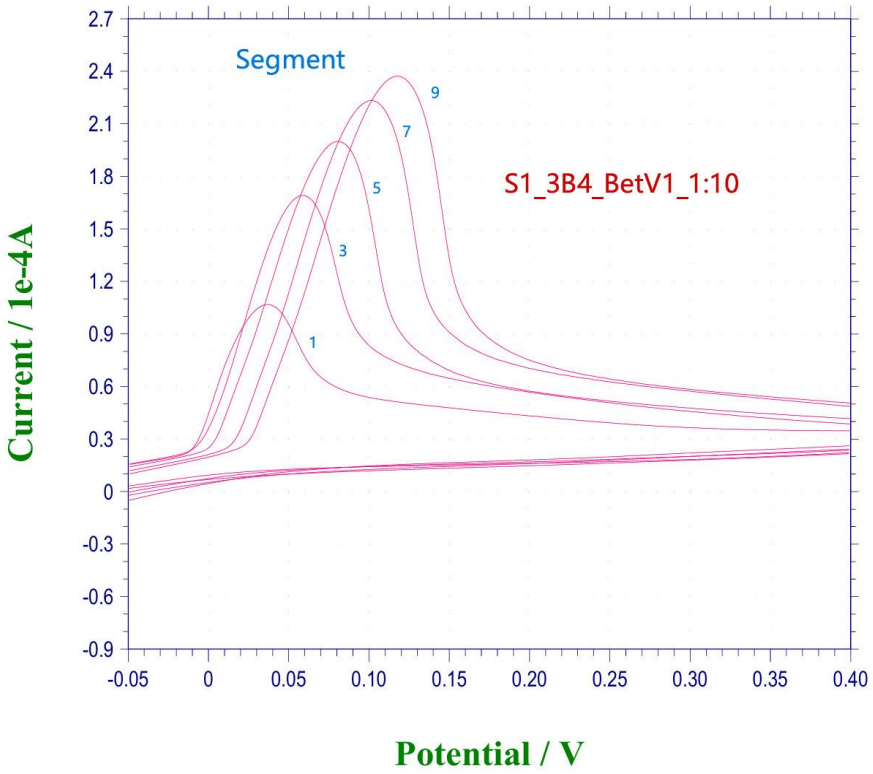

Figure 16. Enlarged view of the positive potential of S1_3B4_Bet v1_1:10.

Table 15. Comparison of positive potential peak areas of S1_3B4_Bet v1_1:10.

Segment	Peak Area Ah (C)	Relative Growth Rate vs. Previous Cycle (%)
1	4.76×10^{-5}	-
3	1.04×10^{-4}	118.5

Continued

5	1.52×10^{-4}	46.3
7	1.88×10^{-4}	23.7
9	2.14×10^{-4}	13.4

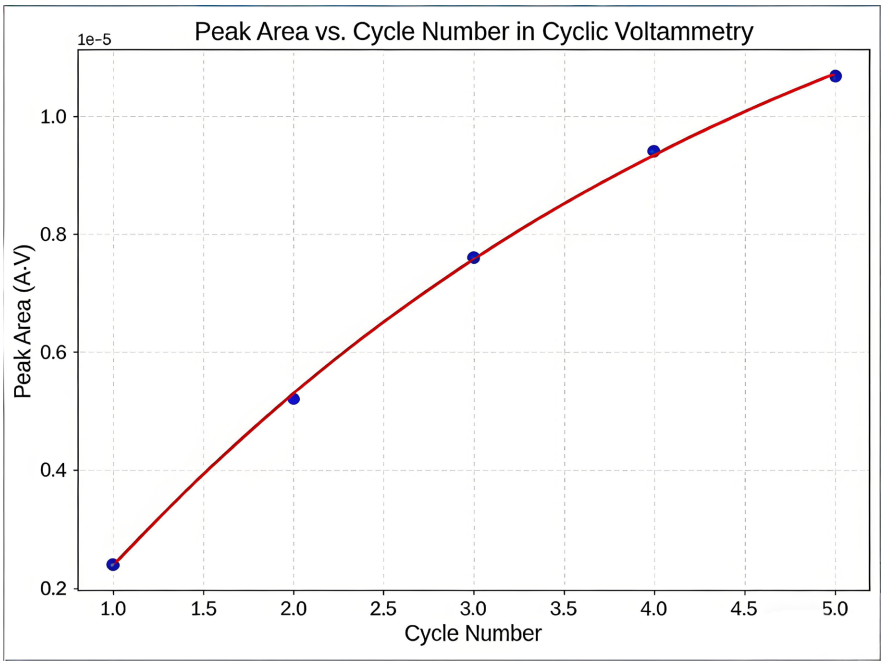

Figure 17. Curve of positive potential peak area vs. cycle number for S1_3B4_Bet v1_1:10.

Figure 17 shows that the peak area increases monotonically with the number of cycles and gradually approaches saturation, reflecting that the antigen-antibody reaction shifts to a stable stage.

3. Results

- In resistance measurement Experimental Group 1, the resistance changes caused by doping with the specific pollen allergen protein in Sensor A, C, E (aver. 1500.883 Ω) are much greater than the resistance changes caused by doping with non-specific pollen allergen proteins in Sensor B, D, F (aver. 576.903 Ω), which preliminarily demonstrated the specific recognition function of the graphene sensor for pollen allergen protein types.
- In resistance measurement Experimental Group 2, the resistance changes caused by doping the graphene sensors with different concentrations of specific pollen allergen proteins increased with the increase of pollen concentration, roughly following the exponential function curve $y = 0.594e^{-239.3x}$, which preliminarily demonstrated the function of the graphene sensor in identifying different pollen allergen protein concentrations.
- To further verify the statistical significance of the concentration-dependent resistivity changes in Experimental Group 2, One-way ANOVA followed by

Tukey's HSD post-hoc test was performed on the $\Delta\rho$ data of 1:5, 1:10, and 1:15 dilutions. The verification results confirm that the resistivity changes of the graphene sensor are significantly dependent on allergen concentration, reinforcing the high R^2 values of the exponential curve fit and validating that the graphene sensor's resistivity changes are not only correlated with allergen concentration but also statistically distinct across tested dilutions. The combined results strengthen the sensor's reliability for quantitative pollen allergen detection

- In the electrochemical verification, the Cyclic Voltammetry (CV) experiment results indicate that the chemically modified graphene electrode can effectively achieve electrochemical recognition of pollen proteins: blank PBS has almost no background peak, proving that the system itself has extremely low interference; obvious redox peaks appear in the specific pollen solution, which increases with the increase of concentration, verifying the correlation between the electrochemical response and the type and concentration of pollen proteins. At the same time, by comparing the potential and peak area changes in different cycle segments, it can be determined that the reaction tends to stabilize after about 10 minutes, providing a reference for the binding mechanism and test time window of the subsequent graphene resistance detection.
- However, electrochemical detection relies on precise, bulky, and high-cost electrochemical workstations, which are more suitable for in-depth revelation of reaction mechanisms and binding processes during the research phase. In practical applications, sensor detection often only needs to focus on the state changes of antigen-antibody binding before and after, rather than tracking the entire reaction process. Therefore, in this study, the graphene sensor still adopts the four-wire method for resistance detection, which can realize real-time monitoring through a simplified circuit and a single-chip microcomputer platform (such as AD5940), making it more portable and low-cost, and more in line with future application needs.

4. Discussion

4.1. Comparison with Existing Biosensing Technologies

This research focuses on a chemically modified graphene biosensor for pollen allergen detection, with experimental results verifying the specific recognition of pollen allergen types and quantitative response to pollen concentrations.

Traditional pollen detection methods suffer from critical shortcomings: manual counting is labor-intensive and low efficiency, while Skin Prick Tests (SPT) are subjective and carry anaphylactic risks. Emerging biosensors for allergens include optical (e.g., surface plasmon resonance, SPR), electrochemical (e.g., gold nanoparticle-based), and piezoelectric (e.g., quartz crystal microbalance, QCM) platforms. The graphene sensor proposed here offers distinct advantages:

- Sensitivity

The four-wire resistance method detects resistivity changes down to 2.16×10^{-6}

Ω·m (1:15 dilution), corresponding to a limit of detection (LOD) ~0.11 mg/mL for ragweed allergen. This is comparable to SPR sensors (LOD ~0.1 mg/mL) but outperforms QCM (LOD ~0.5 mg/mL) and conventional electrochemical sensors (LOD ~0.3 mg/mL). Graphene's 2D structure and high carrier mobility enable femtomolar-level sensitivity (10^{-15} M) for biomolecules, suggesting further optimization (e.g., reduced graphene defects) could lower the LOD to clinically relevant concentrations.

- Specificity

The specific-to-non-specific resistance change ratio (average 1500.88 Ω vs. 576.90 Ω, Experimental Group 1 is ~2.6:1, which is higher than gold nanoparticle-based electrochemical sensors (~1.8:1) and comparable to antibody-functionalized SPR (~3:1). This specificity arises from IgG antibody-antigen recognition and the p-type doping mechanism—non-specific proteins (e.g., birch Bet v1 binding to ragweed antibodies) do not induce Frontier Molecular Orbital (FMO) alignment or significant electron transfer, resulting in minimal resistance changes.

- Portability and Cost

Unlike SPR (>$50 k) or electrochemical workstations (>$10 k), the graphene sensor uses a simplified four-wire circuit and can be integrated with microcontrollers (e.g., AD5940) for real-time monitoring at <$500 per device. This makes it suitable for field deployment (e.g., school-based pollen stations at Beijing No. 80 High School, as implemented in this study) and low-resource settings.

4.2. Implications of Exponential Concentration-Resistivity Relationship

Experimental Group 2 revealed an exponential relationship between pollen concentration and resistivity change ($y = 0.594e^{-239.3x}$, $R^2 > 0.98$), which aligns with Langmuir adsorption kinetics for antibody-antigen binding. At low concentrations (1:15 dilution, binding is diffusion-limited, and small increases in concentration lead to proportional increases in the number of bound combinations, driving a linear rise in resistivity change. At higher concentrations (1:5 dilution), the graphene surface approaches saturation (AFM showed ~80% coverage of allergen-antibody combinations), and additional binding induces cooperative effects, accelerating electron transfer and leading to an exponential increase in resistivity.

This exponential relationship is scientifically meaningful for two reasons:

1) It confirms that the sensor's signal is directly linked to specific binding (not non-specific adsorption), as non-specific interactions would produce a linear or flat response;

2) It enables quantitative detection over a wider concentration range, which covers the typical ambient pollen concentration during allergy seasons. The high R^2 values (>0.98) indicate the model's stability and robustness, supporting future development of a calibration curve for clinical or environmental monitoring.

4.3. Limitations and Future Outlooks

While the sensor demonstrates promising performance, there is still room to im-

prove:

1) The graphene sensors were tested with only two allergens (Ragweed Amb A1, Birch Bet v1); expanding to other common allergens will require optimizing antibody modification for each target.

2) Environmental factors (e.g., humidity, temperature) may affect graphene's conductivity; integrating a humidity/temperature sensor into the device will enable signal correction.

The potential future applications based on this research may include wearable sensors for real-time allergy risk assessment, networked environmental monitoring stations, water quality monitoring and food additives etc. The sensor's low cost and portability also make it suitable for global health initiatives, particularly in regions where traditional pollen monitoring is unavailable.

Acknowledgements

I would like to express my heartfelt gratitude to Professor Lin Xiao, Associate Professor Lu Hongliang, Dr. Han Yechao from the mentorship team of the "China National Science Talent Program" at the University of the Chinese Academy of Sciences (UCAS), as well as Mr. Li Chen, research fellow at Beijing Academy of Science and Technology, for their meticulous guidance and assistance over the past two years.

Originally inspired by the allergy experiences of my mum, this research innovatively applies chemically modified graphene biosensors to the detection of pollen allergens for the first time. Because this research spans across multiple disciplines such as physics, biology, materials science, chemistry, and electronics, it has also received multi-faceted support and assistance during the research process: Special thanks go to Dr. Cao at Peking Union Medical College Hospital for their theoretical guidance in pollen allergy research; Special thanks to Deputy Director Dr. Zhang Hengde from the China Meteorological Administration and Ms. Liu Dan from the Beijing Changping Meteorological Bureau for their selfless sharing of technology in air pollen sampling and manual identification. Without their support, it would not have been possible to complete this research.

Last but not the least, I would also like to thank the teachers and classmates from Beijing No. 80 High School for supporting and assisting me on setting up China's first school-based pollen density monitoring station in campus, which, based on this research, enables sending pollen allergy risks & health advisories to 1800 students and teachers on a daily basis. Since the installation of the monitoring station, the student attendance rate in allergy season has been up by 60%. Thank you all!

Conflicts of Interest

The authors declare no conflicts of interest regarding the publication of this paper.

References

[1] Schmidt, C.W. (2016) Pollen Overload: Seasonal Allergies in a Changing Climate.

Environmental Health Perspectives, **124**, A70-A75. https://doi.org/10.1289/ehp.124-a70

[2] Arbes Jr., S.J., Gergen, P.J., Elliott, L. and Zeldin, D.C. (2005) Prevalences of Positive Skin Test Responses to 10 Common Allergens in the US Population: Results from the Third National Health and Nutrition Examination Survey. *Journal of Allergy and Clinical Immunology*, **116**, 377-383. https://doi.org/10.1016/j.jaci.2005.05.017

[3] Cecchi, L. (2007). Allergenic Pollen and Pollen Allergy in Europe. Allergy. https://doi.org/10.1111/J.1398-9995.2007.01393.X

[4] European Academy of Allergy and Clinical Immunology (EAACI) (2025) Global Atlas of Allergy. European Academy of Allergy and Clinical Immunology.

[5] Muthupalaniappen, L. and Jamil, A. (2021) Prick, Patch or Blood Test? A Simple Guide to Allergy Testing. *Malaysian Family Physician*, **16**, 19-26. https://doi.org/10.51866/rv1141

[6] Babayigit Hocaoglu, A., Cipe, F. and Aydogmus, C. (2015) Are Skin Prick Tests Really Safe? a Case of Anaphylaxis Caused by Skin Prick Testing with Inhalant Allergens. *Allergologia et Immunopathologia*, **43**, 215-216. https://doi.org/10.1016/j.aller.2013.09.011

[7] Stewart, G.A., Peden, D.B., Thompson, P.J. and Ludwig, M. (2012) Allergens and air pollutants. In: Holgate, S.T., Church, M.K., Broide, D.H. and Martinez, F.D., Eds., *Allergy*, Elsevier, 73-128. https://doi.org/10.1016/b978-0-7234-3658-4.00009-3

[8] Oh, J. (2022) Pollen Allergy in a Changing Planetary Environment. *Allergy, Asthma & Immunology Research*, **14**, 168-181. https://doi.org/10.4168/aair.2022.14.2.168

[9] Hao, K., Tian, Z., Wang, Z. and Huang, S. (2020) Pollen Grain Size Associated with Pollinator Feeding Strategy. *Proceedings of the Royal Society B: Biological Sciences*, **287**, Article ID: 20201191. https://doi.org/10.1098/rspb.2020.1191

[10] Scott-Taylor, T.H., Axinia, S., Amin, S. and Pettengell, R. (2017) Immunoglobulin G; Structure and Functional Implications of Different Subclass Modifications in Initiation and Resolution of Allergy. *Immunity, Inflammation and Disease*, **6**, 13-33. https://doi.org/10.1002/iid3.192

[11] Lee, H.O., Treadwell, L.J. and Sun, S. (2022) Understanding the Relationship between Frontier Orbital Level Offsets to Optoelectronic and Electronic Properties of Doped P3ht-Based Composites. *Journal of Materials Science: Materials in Electronics*, **33**, 24276-24284. https://doi.org/10.1007/s10854-022-09148-y

[12] Tang, H., Menabde, S.G., Anwar, T., Kim, J., Jang, M.S. and Tagliabue, G. (2022) Photo-Modulated Optical and Electrical Properties of Graphene. *Nanophotonics*, **11**, 917-940. https://doi.org/10.1515/nanoph-2021-0582

[13] Karthik, P., Vinoth, R., Zhang, P., Choi, W., Balaraman, E. and Neppolian, B. (2018) π-π Interaction between Metal-Organic Framework and Reduced Graphene Oxide for Visible-Light Photocatalytic H_2 Production. *ACS Applied Energy Materials*, **1**, 1913-1923. https://doi.org/10.1021/acsaem.7b00245

[14] Schwarz, F.P., Tello, D., Goldbaum, F.A., Mariuzza, R.A. and Poljak, R.J. (1995) Thermodynamics of Antigen-Antibody Binding Using Specific Anti-Lysozyme Antibodies. *European Journal of Biochemistry*, **228**, 388-394. https://doi.org/10.1111/j.1432-1033.1995.0388n.x

[15] Chandrasekar, N., Balaji, R., Perala, R., Nik Humaidi, N., Shanmugam, K., Liao, Y., *et al.* (2023) A Brief Review of Graphene-Based Biosensors Developed for Rapid Detection of COVID-19 Biomarkers. *Biosensors*, **13**, Article 307. https://doi.org/10.3390/bios13030307

[16] Pinto, H. and Markevich, A. (2014) Electronic and Electrochemical Doping of Graphene by Surface Adsorbates. *Beilstein Journal of Nanotechnology*, **5**, 1842-1848. https://doi.org/10.3762/bjnano.5.195

[17] Kodali, V.K., Scrimgeour, J., Kim, S., Hankinson, J.H., Carroll, K.M., de Heer, W.A., Berger, C. and Curtis, J.E. (2010) Nonperturbative Chemical Modification of Graphene for Protein Micropatterning. *ACS Nano*, **4**, 2218-2224.

[18] Papageorgiou, D.G., Kinloch, I.A. and Young, R.J. (2017) Mechanical Properties of Graphene and Graphene-Based Nanocomposites. *Progress in Materials Science*, **90**, 75-127. https://doi.org/10.1016/j.pmatsci.2017.07.004

[19] Gajhede, M., Osmark, P., Poulsen, F.M., Ipsen, H., Larsen, J.N., van Neerven, R.J.J., *et al.* (1996) X-Ray and NMR Structure of Bet V 1, the Origin of Birch Pollen Allergy. *Nature Structural Biology*, **3**, 1040-1045. https://doi.org/10.1038/nsb1296-1040

[20] Janeway Jr., C.A., Travers, P., Walport, M., *et al.* (2001) Immunobiology: The Immune System in Health and Disease. 5th Edition, Garland Science. https://www.ncbi.nlm.nih.gov/books/NBK27144/

[21] Guo, H.L., Cheng, Y.L., Li, Y. and Guo, X.H. (2023) Analysis and Discussion on the Principles of Cyclic Voltammetry. *University Chemistry*, **38**, 293-300.